

# Using AD5933 IC to Measure Dielectric Constant Variation of Atmospheric Ice

Umair N. Mughal, Beibei Shu

Department of Industrial Engineering, University of Tromsø

Narvik-8505, Norway

e-mail: umair.n.mughal@uit.no, beibei.shu@uit.no

**Abstract** — AD5933 IC is a high precision impedance converter system. In this article, it is used for detection of an atmospheric icing event and to determine atmospheric ice type. A prototype circuit is developed and is tested using a microcontroller AtMega128 clock excitation frequency from 40Hz to 20kHz. The IC is calibrated using a 100kΩ resistor. The real and imaginary components of discrete fourier transform are recorded in order calculate the gain factor at each frequency increment. The unknown impedances are then calculated which are then utilized to calculate the complex dielectric constant of atmospheric ice at each frequency. The results are then compared with the experimental results of Stiles, Evans and Kuroiwa in order to detect an icing event and to determine its type. Results reflect that it is possible to use this approach for detection of an icing event, however it is difficult to determine icing type using this approach.

**Keywords** - AD5933; Atmospheric Ice; Conductivity; Dielectric Constant; Dissipation Factor; Frequency Sweep.

## I. INTRODUCTION

The aim of this article is to evaluate the usage of AD5933 Integrated Circuit (IC) to detect an atmospheric icing event and determine ice type. Using a pre-defined frequency range, this IC measure the real and imaginary components of discrete fourier transform of the load impedance. These components are recorded in order to calculate the gain factor at each frequency which is then utilized to determine the unknown impedances. In this experimental investigation, the load impedance is atmospheric ice. The calculated load impedances are utilized, to calculate capacitance of atmospheric ice at each excitation frequency. This capacitance measurement technique was highlighted in state of the art review by Mughal et. al. [1] and Homola et. al. [2], to be one of the many possible measurement techniques to detect atmospheric icing event, icing type and icing rate.

This article is divided in five sections. Section I is an introduction. Section II is the state of the art, which is further divided in three sections in order to understand atmospheric ice capacitance measurement technique using frequency sweep approach and application/construction of AD5933 IC. Section III is about the approach and architecture of the circuit developed to measure capacitance of atmospheric ice. Section IV describes the experimental results and discussions. Section V is the last section which includes conclusions and limitations to use this IC.

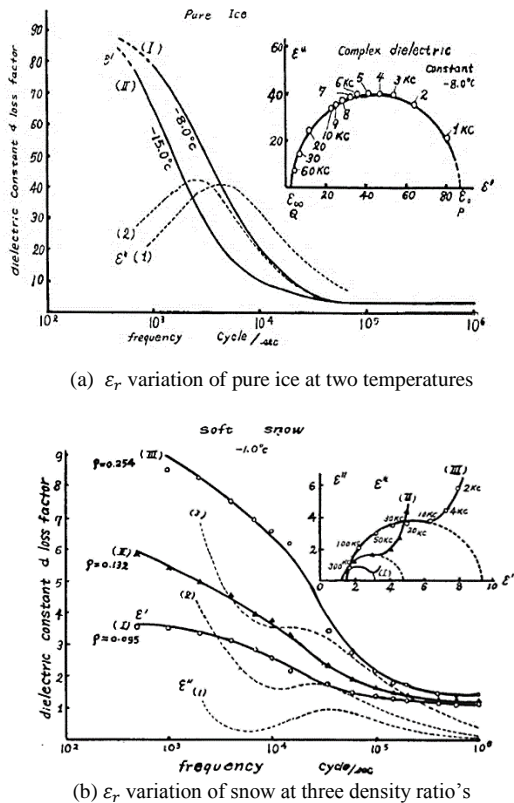
## II. STATE OF THE ART

### A. Capacitance Measurement Using Frequency Sweep:

Capacitive ice sensors generate an electric field to detect the presence of dielectric materials. An electric field radiates outward around the probe and a dielectric material in close proximity of the field affects the measured capacitance. Capacitance  $C = C_0 \epsilon_0 \epsilon_r$  can be measured by the variation in relative permittivity or dielectric constant ' $\epsilon_r$ ' or by the variation in electrode geometry ' $C_0$ '. Where  $C_0 = A/d$  where A is the area of the electrode and d is the distance between the electrodes,  $\epsilon_0$  is the permittivity of vacuum equal to  $8.85 \times 10^{12} F/m$ .

Water molecule is polar in nature due to electronegativity difference of 1.2 between hydrogen and oxygen. These polar molecules orient themselves with the electrical field. However, when the electrical field is removed they disorient themselves. Under the influence of electric field, polar molecule behave like a parallel combination of capacitor and resistor. The dielectric constant of these molecules  $\epsilon_r(\omega) = \epsilon_r'(\omega) - j\epsilon_r''(\omega)$  is a complex number, which is dependent upon the excitation frequency. Here  $\epsilon_r'$  represents the amount of energy from the electric field, which is stored in the material and  $\epsilon_r''$  represents how lossy or dissipative a material is to the external electric field. This loss factor  $\epsilon_r''(\omega)$  includes the effects of both dissipation and conductivity. Also, the relative loss of the material is the ratio of energy lost to the energy stored and is defined as 'dissipation factor  $D = \tan \delta = \epsilon_r''/\epsilon_r'$ '. Polar materials generally have many dielectric mechanisms (atomic, electronic and dipolar) in different frequency domains associated with a cutoff frequency in each domain, which appears as a peak in  $\epsilon_r'' = \epsilon_r''(\omega)$  (likewise  $D = D(\omega)$ ) curve. The dipolar orientation is generally associated with the relaxation phenomenon, whereas the electronic and atomic polarization are associated with the resonance phenomenon. In the frequency domain analysis, the relaxation frequency ' $f_c$ ' is indicative of the relaxation time,  $\tau_0 = 1/2\pi f_c$ . This frequency can be detected by a peak by sweeping the excitation frequency and is generally unique for different materials. If we replace  $\epsilon(\omega \rightarrow 0) = \epsilon_s$  and  $\epsilon(\omega \rightarrow \infty) = \epsilon_\infty$ , then by varying excitation frequencies, the dielectric constant of polar material can be analytically described by Debye relation, see (1) and Figure 1.

$$\epsilon(\omega) = \epsilon_{\infty} + \frac{\epsilon_s - \epsilon_{\infty}}{1 + j\omega\tau} \tag{1}$$



(a)  $\epsilon_r$  variation of pure ice at two temperatures

(b)  $\epsilon_r$  variation of snow at three density ratio's

Figure 1. Visualization of Debye Relations [3]

**B. Dielectric Constant of Atmospheric Ice**

Figure 1a shows the dielectric constant variations of a sample of pure ice at two different temperatures ( $-8^{\circ}C$  and  $-15^{\circ}C$ ). Both curves of  $\epsilon'_r(\omega)$  and  $\epsilon''_r(\omega)$  are shifting towards left as temperature was decreasing. The relaxation frequency ' $f_c$ ' was in the range of  $1 \rightarrow 10kHz$  where the value of  $\epsilon''_r(\omega)$  is in the range of  $40 \rightarrow 50$ . Also, Figure 1b shows the dielectric constant variations of three distinct samples of snow with density ratios  $\rho = 0.095, 0.132$  and  $0.254$ . Both curves of  $\epsilon'_r(\omega)$  and  $\epsilon''_r(\omega)$  are increasing in magnitude as the density ratio's are increasing. The low frequency deviation of these curves from the ideal semi circle behavior (in Argand Diagram) is due to the conductivity of snow, which is increasing with increasing density ratio's. However, the relaxation frequency ' $f_c$ ' was not quite distinct but it lie in the range of  $10 \rightarrow 100kHz$  where the value of  $\epsilon''_r(\omega)$  are under 4 for all density ratio's. The application of the electrical properties to the measurement of ice thickness, temperature, crystal orientations are also presented in Evans [4]. It is mentioned in Sihvola et. al. [5] that for dry snow, the dielectric constant is determined by the density and for wet snow, the imaginary part and the increase of the real part due to liquid water have the same volumetric wetness dependence. In Sihvola et. al. [5], the results indicate that the complex dielectric constant is practically independent of the

structure of snow. The static dielectric constants  $\epsilon_{rs}$  of both polycrystalline and single crystals of ice have been carefully determined, Auty and Cole [6].

Furthermore, Weinstein [7] and Jarvinen [8] proposed two different capacitive based ice detection methods. In his patent [8], Jarvenin has proposed the use of AD5933 to detect icing event, icing type, ice thickness and icing rate, however no commercially available sensor is found to utilize this technique for measurement of atmospheric icing parameters.

**C. AD5933 IC and its usage**

AD5933 is a smallest and lowest power solution to measure the range of impedances using discrete fourier components. The general impedance measurement system can be seen in Figure 2. The system is excited by a range of frequencies in order to measure the output phase and impedance magnitude. This approach is called the frequency domain measurement technique [9].

In the block diagram from Figure 3, a direct digital synthesizer or DDS (AD9834) is used to generate a predefined frequency sweep to a tuning resolution of  $0.1Hz \rightarrow 100kHz$ . The output frequency is then filtered and amplified before being applied to the known impedance. Analog to digital converter (ADC) is then utilized to sample synchronously across all frequencies so as both the excitation and response waveform can be compared to allow full phase information. The data is then delivered to digital signal processing (DSP) block for further processing.

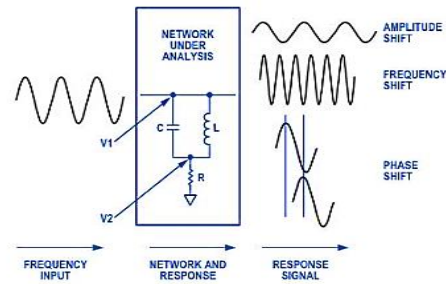


Figure 2. General Impedance Measurement System [10]

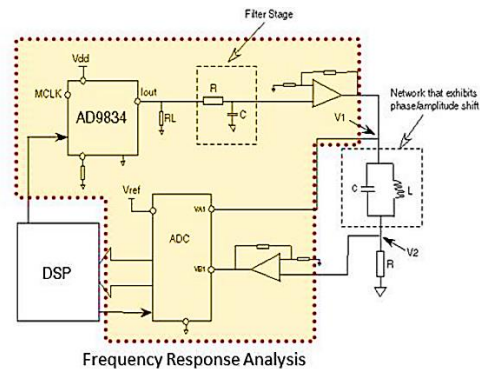


Figure 3. Integrated single chip solution [10]

AD5933 IC have been commercially utilized in impedance spectroscopy, proximity sensing, chemical analysis, bio medical analysis, human body impedance analysis and corrosion analysis. Norbotten B. J. [11] used AD5933 in the frequency range of 5 → 100kHz and measured human body impedance in the range of 0.1kΩ → 10MΩ. Similarly Pena A. A. [12] developed spectrometer for electrical bioimpedance using this IC. This IC has also been utilized for measuring blood glucose levels by Kamat et. al. [13].

III. APPROACH AND ARCHITECTURE

The frequency generator allows an external complex impedance to be excited with a known frequency. The frequency generator require three inputs, which are start frequency 'F<sub>START</sub>', incremental frequency 'ΔF' and number of frequency increments 'N<sub>INCR</sub>', see Figure 4.

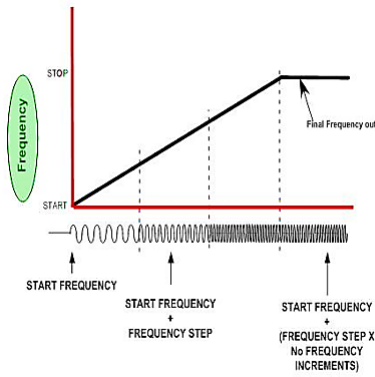


Figure 4. Frequency sweep characteristics

The microcontroller used to program and to implement the architecture was Atmega128 due to its memory. Also, this microcontroller had the flexibility to read/write on AD5933 IC's internal registers through I<sup>2</sup>C interface. Nevertheless, the I<sup>2</sup>C address of AD5933 was fixed by the manufacturer. In this experiment it was desired to sweep the frequency from 40Hz → 20kHz for a step of 40Hz. In order to meet this requirement, a changeable clock signal for AD5933 IC, was generated through Atmega128 timer1 in Clock Timer Counter (CTC) mode, see Figure 5. In CTC mode the counter was cleared to zero, when the free running counter or a 16 bit register (TCNT1) matches either the output compare register OCR1A (WGM13:0 = 4 where WGM is wave generation mode) or the input capture register ICR1 (WGM13:0 = 12). The counter value (TCNT1) was increased until a compare match occurs with either OCR1A or ICR1, and then counter (TCNT1) was cleared, see Figure 6.

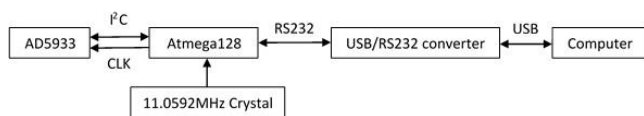


Figure 5. Block diagram for communication path

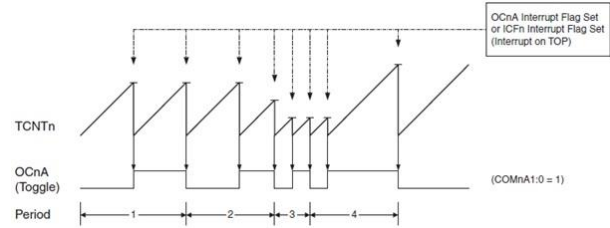
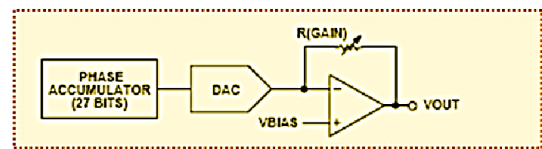
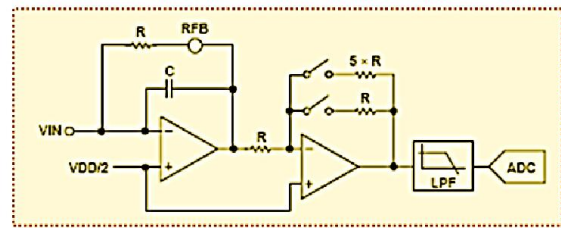


Figure 6. CTC mode, timing diagram

The function of timer1 over here was to generate frequencies, so that the CTC interrupt should be disabled to save CPU cycles. This Alf and Vegard RISC processor (AVR) timer was connected to general I/O Port. Then general I/O pin PD5 was converted to compare match output OC1A. After that OC1A pin function was set to toggle on compare match. Then the fuse bits were programmed to make clock division factor to 1 and set the timer1 clock source to no prescaling. Hence, the timer clock source was equal to crystal frequency,  $clk_{I/O} = 11.0592\text{MHz}$ . The output frequency was  $f_{out} = clk_{I/O} / (2 \times OCR1A)$ . OCR1A was a 16-bits register, which ranged from 1 to 65535 therefore the range of output frequency could be  $clk_{I/O} / (2 \times 1)$  to  $clk_{I/O} / (2 \times 65535)$ , that is, from 5.5296MHz to 84Hz. Therefore when the system was running, the only requirement was to change the value of OCR1A to change the output frequency. Therefore using an internal clock source, which was 16.776MHz, the AD5933 chip could measure the impedance spectrum in the required frequency range of 1 kHz–100kHz. However, using external clock source (as applied in this work), which was generated by AVR, the frequency range can go lower than 1 kHz.



(a). Transmit Stage



(b). Receive Stage

Figure 7. Transmit Stage and Receive Stage of AD5933 [10]

This IC worked in two stages, which are transmit stage and receive stage. The transmit stage of the AD5933 was made up of a 27 bit phase accumulator DDS core, which provided the output excitation signal at a particular frequency, see Figure 7a. The input to the phase accumulator was taken from the contents of the start frequency register

(Ram locations 82h, 83h and 84h). Although the phase accumulator offers 27bits of resolution, the start frequency register had the 3 most significant bits (MSBs) sets to 0 internally; therefore it became possible to program only the lower 24bits of the start frequency register. The frequency resolution 0.1Hz could be achieved. The frequency resolution was programmed via a 24 bit word loaded serially over the I<sup>2</sup>C interface to the frequency increment register. The last input was number of increments.

The receive stage comprised of a current to voltage amplified, followed by a programmable gain amplifier (PGA), an anti aliasing filter, and an ADC, see Figure 7b. The unknown impedance was connected between the V<sub>OUT</sub> and V<sub>IN</sub> pins. The first stage current to voltage amplifier sat the V<sub>IN</sub> pin as a virtual ground with a DC value of V<sub>DD</sub>/2. The signal current developed across the unknown impedance was then flowed into the V<sub>IN</sub> pin, which, developed a voltage signal at the output of the current to voltage converter.

The gain of the current to voltage amplifier was determined by selecting a feedback resistor of  $Z_{calibrated} = 100k\Omega$  connected between rectified feedback (RFB) and V<sub>IN</sub>. The aim was to maintain the signal within the linear range of ADC (0V to 3.3V analog positive supply voltage or AVDD). The gain setting was set to one. The signal was then sent through a low pass filter and was presented to the input of the 12bit, 1 mega samples per second (MSPS) ADC.

The response signal from the impedance was sampled by the on-board ADC and discrete fourier transform (DFT) processed by an on-board DSP engine. The DFT algorithm returned real 'R' and imaginary 'I' data-word at each frequency point along the frequency sweep. Using these 'R' and 'I', magnitude 'M' and phase 'φ' were calculated using (2) and (3). Therefore  $M_{calibrated}$  and  $\varphi_{calibrated}$  were measured using  $R_{calibrated}$  and  $I_{calibrated}$ . Atmospheric ice was then placed on the electrode for which  $M_{unknown}$  and  $\varphi_{unknown}$  were measured using  $R_{unknown}$  and  $I_{unknown}$ .

$$M = \sqrt{R^2 + I^2}, \quad (2)$$

$$\varphi = \tan^{-1} (I/R). \quad (3)$$

It was also necessary to ensure that the signal was always maintained within the linear range of the ADC over the impedance range of interest. Before measuring the unknown impedance, the calibration must be done. In calibration stage, the manufacturer mentioned that a gain factor needs to be calculated. The gain factor 'GF' could be calculated using,

$$GF = \frac{1}{Z_{calibrated} \times M_{calibrated}}. \quad (4)$$

However, in this analysis, there was no need to calculate the gain factor due to the reason that in the measuring stage, the unknown impedance ' $Z_{calibrated}$ ' and its unknown phase were calculated using,

$$Z_{unknown} = \frac{Z_{calibrated} \times M_{calibrated}}{M_{unknown}} \quad (5)$$

$$\varphi_{unknown} = \text{atan} \left( \frac{I_{unknown}}{R_{unknown}} \right) - \text{atan} \left( \frac{I_{calibrated}}{R_{calibrated}} \right) \quad (6)$$

As capacitance  $C = 1/2\pi fZ$ , therefore using (5) and (6) in complex dielectric constant equation, we derive,

$$\varepsilon_r' - j\varepsilon_r'' = \frac{1}{2\pi j f C_0 \varepsilon_0 Z_{unknown} \exp(\varphi_{unknown})} \quad (7)$$

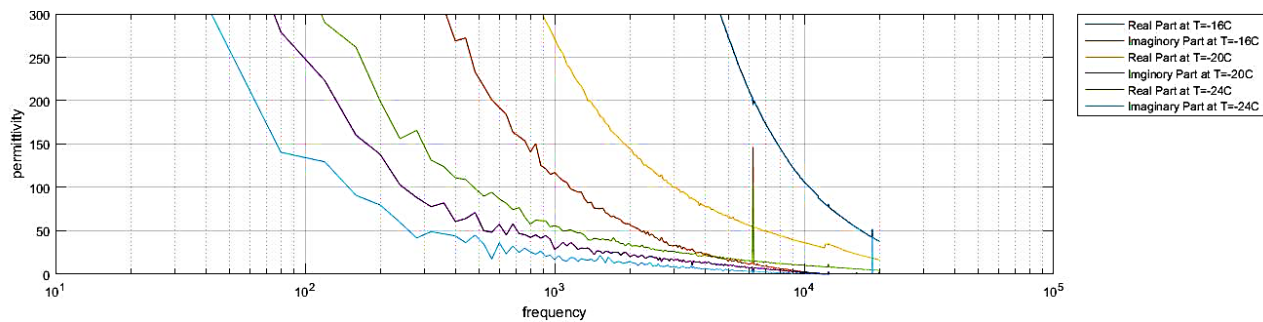
Equation (7) is then further utilized to determine the dielectric constant of the unknown sample of atmospheric ice.

#### IV. EXPERIMENTAL RESULTS AND DISCUSSIONS

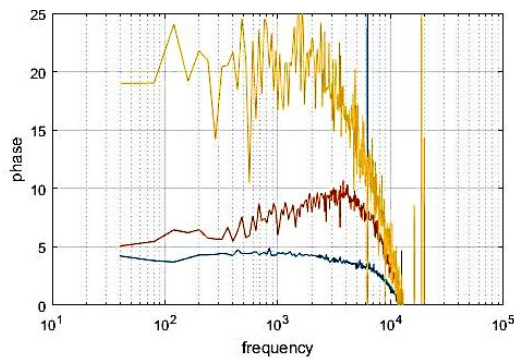
Using (7), the results of  $\varepsilon_r'$  and  $\varepsilon_r''$  were obtained by writing a simple algorithm in MatLab. The experimentations were done in the Cold Climate Chamber of UiT Campus Narvik, using the following samples at the respective temperatures,

- i. Glaze ice frozen on the electrode plate at a temperature of -16<sup>o</sup>C,
- ii. Glaze ice frozen on the electrode plate at a temperature of -20<sup>o</sup>C,
- iii. Glaze ice frozen on the electrode plate at a temperature of -24<sup>o</sup>C,
- iv. Natural Snow from ground outside university campus at a temperature of -3<sup>o</sup>C.
- v. Normal tap water at a temperature of 26<sup>o</sup>C,

The results of glaze ice at three different temperatures can be seen in Figure 8. This figure indicates there was no prominent peak observed in the dielectric constant variation ( $\varepsilon_r'' =$  imaginary part) with the variation in frequency (Figure 8a), hence it was not possible to compare the results of Stiles [3] and Kuroiwa [14]. Both curves of  $\varepsilon_r'(\omega)$  and  $\varepsilon_r''(\omega)$  were shifting towards left as temperature was decreasing. However, the capacitance phase ( $\text{atan}(\varepsilon_r''/\varepsilon_r')$ ) or dissipation factor ( $\varepsilon_r''/\varepsilon_r'$ ) reflect an observable trend. In the frequency range of 1 → 10kHz (relaxation frequency ' $f_c$ '), the variation in the phase is prominent (Figure 8b). This value of  $f_c$  was found in agreement with the experimental results of Stiles (Figure 1). It was also found that the average value of this phase reached a relative maximum of 20<sup>o</sup> by decreasing the temperature from -16<sup>o</sup>C → -24<sup>o</sup>C, hence more capacitance. The results were however very noisy possibly due to some harmonics from the microcontroller and reasonably high conductance of the sample. In another test, the results were compared with the natural occurring snow, collected from outside the university campus and water samples. The results are shown in Figure 9. These results also indicated the same trend in the dielectric constant variation ( $\varepsilon_r'' =$  imaginary part) with frequency (Figure 9a), hence it was not possible to determine the relaxation due to dominated noise. Similarly, it was found that the phase of the capacitance ( $\text{atan}(\varepsilon_r''/\varepsilon_r')$ ) reflect observable trend for samples of glaze ice, snow and water (Figure 9b).

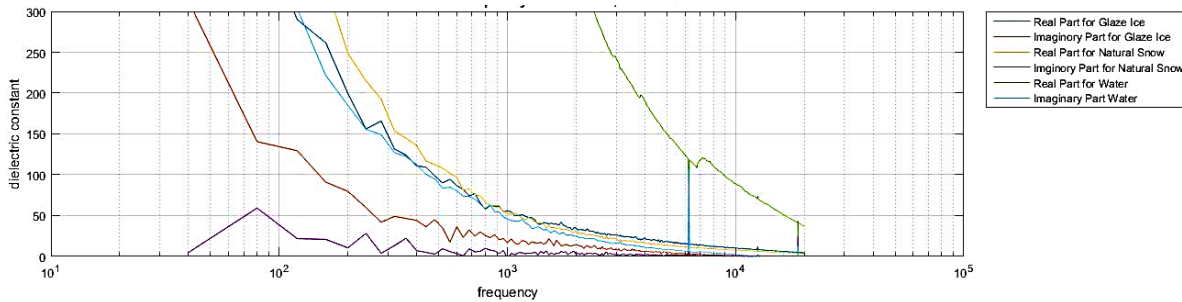


(a). Dielectric constant ( $\epsilon_r' = real, \epsilon_r'' = imaginary$ ) variation with frequency

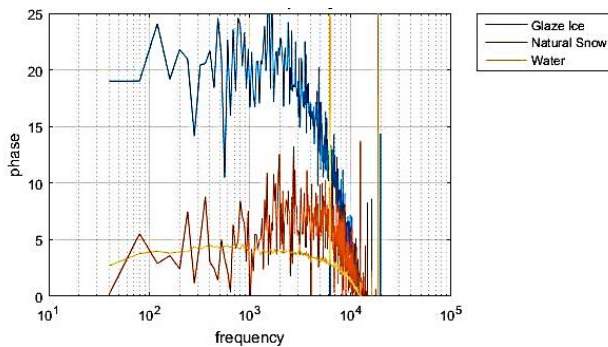


(b). Dielectric constant phase ( $atan(\epsilon_r''/\epsilon_r')$ )

Figure 8. Dielectric constant variation with excitation frequency for Glaze Ice frozen on the electrode plate at temperatures -16°C, -20°C and -24°C [15]



(a). Dielectric constant ( $\epsilon_r' = real, \epsilon_r'' = imaginary$ ) variation with frequency



(b). Dielectric constant phase ( $atan(\epsilon_r''/\epsilon_r')$ )

Figure 9. Dielectric constant variation with excitation frequency for glaze ice at -24°C, natural snow at -4°C and water sample at 24°C [15]

V. CONCLUSION AND FUTURE WORK

AD5933 IC works upon the frequency domain capacitance measurement technique [9]. It was possible to use the dissipation factor for detecting an icing event using the approach utilized in this experimental study. Most of the existing experimental study [3] [4] [14], by sweeping the frequency to determine the dielectric variation in different type of atmospheric ice, are laboratory based. However, the aim in this article was to evaluate the usage of AD5933 IC to detect an atmospheric icing event and determine ice type. It was found that the scope to utilize the excitation frequency from microcontroller clock for AD5933 IC is limited. A lot of noise was observed in the values of complex dielectric constant due to this and values were found possibly due to unwanted harmonics. It was therefore not possible to compare these values with the experimental values of Stiles and Ulaby [3], Evans [4] and Kuroiwa [14]. It was found that the average value of this phase reached a relative maximum of  $20^0$  by decreasing the temperature from  $-16^0C \rightarrow -24^0$ , hence more capacitance. Nevertheless, by recording the dissipation factor / phase value, it was found possible to at least detect an icing event. Also due to reasonably high conductivity of ice, the complex dielectric constant was continuously reducing even at same environmental conditions, however the dissipation factor remained stable for longer range of frequencies.

For future experimentations, it will be useful to improve the outputs of AD5933 IC for measuring atmospheric icing parameters by utilizing the methods as described by Leonid [16].

ACKNOWLEDGMENT

The work was funded by Research Council of Norway Project No. 195153 (ColdTech RT3), Norwegian Centre for International Cooperation in Education Project No. HNP-2014/10023 and WindCoE (Nordic Wind Energy Centre) project funded within Interreg IVA Botnia-Atlantica, as part of European Territorial Cooperation (ETC).

REFERENCES

[1] U. N. Mughal, M. S. Virk, and M. Y. Mustafa, "State of the Art Review of Atmospheric Icing Sensors," *Sensors and Transducers*, vol. 198, pp. 2-15, 2016.

[2] M. C. Homola, P. J. Nicklasson, and P. A. Sundsbo, "Ice sensors for wind turbines," *Cold Regions Science and Technology*, vol. 46, pp. 125-131, 2006.

[3] W. H. Stiles and F. T. Ulaby, "Dielectric properties of snow," *Journal of Geophysical Research*, vol. 85, pp. 91-103, 1981.

[4] S. Evans, "Dielectric properties of ice and snow - a review," *Journal of Glaciology*, vol. 5, pp. 773-792, 1965.

[5] A. Sihvola, E. Nyfors, and M. Tiuri, "Mixing formulae and experimental results for the dielectric constant of snow," *Journal of Glaciology*, vol. 31, pp. 163-170, 1985.

[6] R. P. Auty and R. H. Cole, "Dielectric Properties of Ice and Solid D<sub>2</sub>O," *Journal of Chemical Physics*, vol. 20, pp. 1309-1314, 1952.

[7] L. M. Weinstein, "Ice Sensor," 1988.

[8] P. O. Jarvinen, "Total impedance and complex dielectric property ice detection system," 2008.

[9] K. Kao, *Dielectric Phenomena in Solids*, 2004.

[10] A. Devices. (2016, March 14th). *AD5933 Impedance to Digital Converter*. Available: <http://dkc1.digikey.com/us/en/TOD/ADI/AD5933/AD5933.html>

[11] B. J. Nordbotten, "Bioimpedance Using the Integrated Circuit AD5933," Master of Science, Department of Physics, University of Oslo, 2008.

[12] A. A. Pena, "A Feasibility Study of the Suitability of an AD5933 based spectrometer for EBI Applications," Electronic Instrumentation, University of Boras, 2009.

[13] D. K. Kamat, B. Dhanashri, and P. M. Patil, "Blood Glucose Measurement Using Bioimpedance Technique," *Advance in Electronics*, vol. 2014, 2014.

[14] D. Kuroiwa, "The dielectric property of snow," *Union Geodesique et Geophysique International* vol. Association Internationale de Hdrologie Scientifique, Assemblée generale de Rome., pp. 52-63, 1956.

[15] U. N. Mughal, B. Shu, and T. Rashid, "Proof of Concept of Atmospheric Icing Sensor to detect icing, determine icing type and measure melting rate," *Submitted in IEEE Transactions on Dielectrics and Electrical Insulation, Paper ID 6048*, 2016.

[16] L. Matsiev, "Improving Performance and Versatility of Systems Based on Single-Frequency DFT Detectors Such as AD5933," *Electronics*, vol. 4, pp. 1-34, 2015.